Transient switching dynamics between asynchronous and synchronous modes in a bidirectional ultrafast fiber laser

Chao Wang,[1,2,*] Yujia Li,[1,2,*] Dongmei Huang,[1,2,†] Hongjie Chen,[1,2] Yihuan Shi,[1,2] and Feng Li[2,3]

[1]*Photonics Research Institute, Department of Electrical Engineering, The Hong Kong Polytechnic University, Hong Kong SAR, China*

[2]*The Hong Kong Polytechnic University Shenzhen Research Institute, Shenzhen 518057, China*

[3]*Photonics Research Institute, Department of Electronic and Information Engineering, The Hong Kong Polytechnic University, Hong Kong SAR, China*

(Received 20 February 2022; accepted 5 April 2022; published 21 April 2022)

Continuous interest in bidirectional ultrafast fiber lasers not only reinforces the practical applications in coherent dual-comb spectroscopy but also enriches the understanding of soliton dynamics in nonlinear systems. However, the transient dynamics of bidirectional solitons are still unexplored. Here, we report on an observation of the switching dynamics in a net-anomalous-dispersion bidirectional ultrafast fiber laser which can operate in both asynchronous and synchronous operations. Transient switching dynamics between the asynchronous and synchronous states are demonstrated, which is accompanied by switchable and weak interaction between bidirectional solitons. The dynamical evolution and output properties of the asynchronous and synchronous bidirectional solitons are investigated respectively. Stable breathing solitons in the synchronous operation show opposite behaviors in both spectra and pulse energy dynamics, which vary with different pump powers. Our findings provide insight into the transient dynamics in ultrafast lasers and contribute to the understanding of nonlinear systems in general.

DOI: 10.1103/PhysRevA.105.043515

I. INTRODUCTION

Optical soliton dynamics in ultrafast fiber lasers have recently been broadly investigated ranging from fundamental physical mechanisms to practical applications such as variation sensing [1,2]. In the past, the experimental study of soliton dynamics is challenging since it is difficult to resolve the temporal and spectral features. Benefiting from the time stretch dispersive Fourier transform (TS-DFT) technology which stretches an optical pulse in a dispersive medium by cumulating a group-velocity dispersion (GVD) large enough to map the optical spectrum into the temporal domain, a single short spectrum with an update frame of several tens of megahertz is possible [3]. Such a real-time approach helps scientists to experimentally observe versatile soliton dynamics, such as soliton buildup [4], rouge waves [5], soliton molecules [6], soliton interactions [7,8], and soliton explosions [3] in ultrafast lasers and nonlinear systems. All these studies have substantially enriched the knowledge of soliton evolutions and dynamics in ultrafast optics.

Especially, bidirectional fiber laser is the promising light source for dual-comb generation and applications [9–12]. Also, two pulse trains collide with each other every round trip, offering a special and excellent platform for exploring complex dynamics of solitons. The soliton dynamics in the bidirectional fiber lasers highly depend on the net cavity dispersion. In the net-normal-dispersion regime, similar soliton behaviors with spectral and temporal characteristics were observed in the buildup process of synchronous operation [13]. Meanwhile, the explosion dynamics in breathing dissipative solitons were also explored, showing high behavior similarity and dissipative rogue waves during the buildup process [14]. In the net-anomalous-dispersion regime, the counter-propagating pulses experience independent dynamics during the whole buildup process, which is opposite to the results in the net-normal-dispersion regime [15]. In addition, the bidirectional fiber laser can operate in asynchronous and synchronous modes with different and same repetition rates, respectively [16]. The buildup dynamics, soliton explosion, and mutually induced soliton polarization instability of bidirectional solitons have been demonstrated [17]. So far, the switching dynamics between the asynchronous and synchronous states are still unexplored.

In this work, we report on an observation of the transient dynamics between the asynchronous and synchronous states in the bidirectional ultrafast fiber laser operating in the net-anomalous-dispersion regime. Utilizing the TS-DFT technology, the whole spectral evolutions of both the stable and switching operations in asynchronous/synchronous modes are investigated. Section II demonstrates the experimental setup of the bidirectional ultrafast fiber laser. Then the detailed spectral evolution and dynamics of the asynchronous and synchronous operations are studied in Sec. III. Section IV concludes the whole paper.

II. EXPERIMENTAL SETUP

The experimental setup is depicted in Fig. 1. The bidirectional fiber laser operating in the C band is passively mode-locked based on the CNT (carbon nanotube) as the

*These authors contributed equally to this work.

†Corresponding author: meihk.huang@polyu.edu.hk

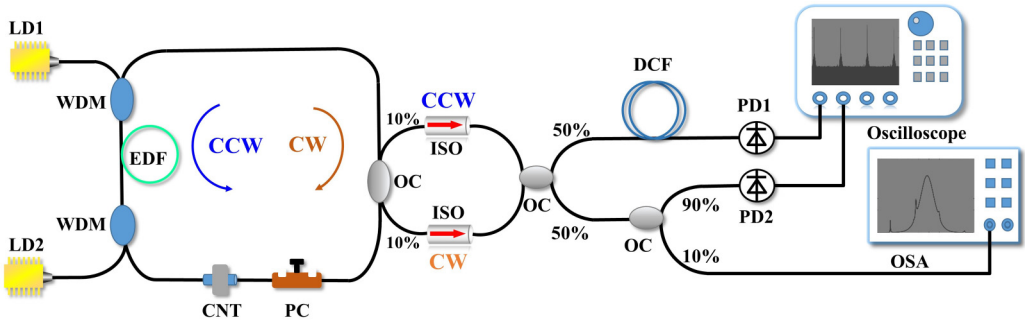

FIG. 1. Schematic setup of the bidirectional fiber laser and the measurement. LD: laser diode. OC: optical coupler, PC: polarization controller, ISO: isolator, WDM: wavelength division multiplexer, CNT: carbon nanotube-based saturable absorber, EDF: Erbium-doped fiber, DCF: dispersion compensation fiber, PD: photodetector, OSA: optical spectrum analyzer.

saturable absorber. The fiber cavity consists of 1 m erbium-doped fiber (EDF, Er30-4/125, Liekki) with a GVD parameter of about $+14.45\,\mathrm{ps}^2/\mathrm{km}$ and ∼3.8-m single-mode fiber (SMF28e) with a GVD parameter of $-22\,\mathrm{ps}^2/\mathrm{km}$. The fiber laser operates in the anomalous dispersion regime with a net cavity dispersion of about $-0.069\,\mathrm{ps}^2$. The EDF is pumped through two 980/1550 wavelength division multiplexers by two 976-nm laser diodes in opposite directions, offering a gain balance between two directions for simultaneous mode-locking operation. An optical coupler is used to extract 10% power in each direction for output. A polarization controller is inserted into the cavity to optimize the polarization state and adjust the output properties. The whole length of the laser cavity is about 4.79 m, suggesting a repetition rate of about 43.32 MHz. Two isolators are used after the 10% OC to avoid the backward reflective light which would affect the stable operation of the cavity. A 50:50 OC combines the bidirectional pulses for consistent and synchronous analysis. The temporal intensity pattern is detected by a photodetector (PD2) with 43 GHz bandwidth and captured by a real-time oscilloscope (OSC, Keysight, DSAX96204Q) with 1 Gs/s sampling rate, while the average spectra are captured by an optical spectrum analyzer (OSA, Yokogawa AQ6370D) with 0.05-nm resolution.

To investigate the real-time dynamics of the bidirectional fiber laser, the TS-DFT method is used with a spool of dispersion compensating fiber (DCF, DSCM-10-C, OFS) with -168.2 ps/nm dispersion and detected by a 43 GHz photodetector (PD1, FinisarBPDV2120R). Benefiting from the real-time OSC with a high sampling rate of 40 GHz, we can take simultaneous measurements of the output pulses with a temporal and spectral resolution of 25 ps and ∼0.36 nm, respectively.

III. EXPERIMENTAL RESULTS AND DISCUSSION

Usually, a light signal in one direction can obtain sufficient gain to form a mode-locking operation, while it is suppressed in the other direction. However, by optimizing the pump power and polarization state, mode-locking operations in both directions can be achieved. In this paper, by precisely adjusting the pump power and the polarization state of the light, both asynchronous and synchronous mode-locking operations are achieved. More interestingly, the transient switching dynamics between the asynchronous and synchronous states are observed in a bidirectional mode-locked laser, which will be presented from both the statical and dynamical aspects.

A. Transient switching dynamics between synchronous and asynchronous mode-locking operations

Firstly, we gradually increase the pump power and find an appropriate pump power under which both synchronous and asynchronous operations can be independently achieved by adjusting the PC. Then, by precisely adjusting the PC in the intermediate state, the transient switching mode between the synchronous and asynchronous operations is detected and acquired by the OSA and the OSC. The audio-visual record is also shown in the Supplemental Material [18]. The pump powers of LD1 and LD2 are 26 and 12 mW, respectively. To observe the dynamics of the transient switching process, the TS-DFT technique is used to capture the shot-to-shot spectral evolution. In the experiment, we use a low sampling rate to measure the switching process by recording more round trips since the transient switching randomly happens. The simultaneous measurements of the spectra over two million round trips with a sampling rate of 10 GHz are presented. Figure 2(a) shows the three-dimensional (3D) view of the spectral evolution involved in the transient switching process. Benefitting from the shot-to-shot spectral measurement with the TS-DFT technique, it can be observed that the bidirectional laser operated in the asynchronous mode most times and randomly switched to the synchronous mode for a short time. Two spectra of CW and CCW pulses periodically approach and separate with each other with constant steps in the asynchronous mode. The energy will gradually increase when two solitons are approaching each other and will reach the peak value when they exactly overlapped. Oppositely, the energy will decrease when two solitons are walking off. However, for synchronous operation, the energy of two solitons keep constant in a parallel mode. From the top view of the spectral evolution in Fig. 2(b), we can precisely observe when and how long the switching process has happened. The operation in synchronous mode lasts about 400 000 round trips, responding to about 9-ms continuous operation.

To further look inside the fine dynamics in the switching process, the real-time OSC with a higher sampling rate of 40 GHz is used, resulting in a spectral resolution of about

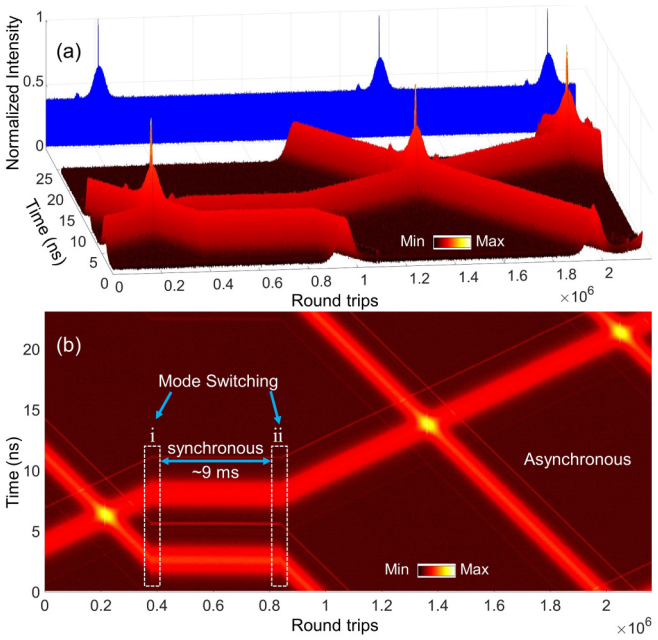

FIG. 2. (a) 3D view of the spectral evolution in CW and CCW directions involves the transient switching. The blue (upper) trace represents the front view of the spectral evolution trace. (b) The top view of the spectral evolution (Region i and ii represent the switching process).

0.36 nm. We are lucky to capture this full process in 500 000 round trips after many times randomly triggering. Figure 3(a) shows the spectral evolution involving the transient switching dynamics. The bidirectional laser stably operates in the asynchronous mode and switches to the breathing synchronous mode. The breathing solitons collide every round trip and interact with each other for energy exchange in a constant period. The switching is probably caused by the random change in the gain or nonlinearity induced by the fluctuation of polarization state and pump power. The breathing operation lasts about 3 ms and then breaks back to the asynchronous operation. The zoom-in views of three key regions in Fig. 3(a) are dedicated in Figs. 3(b)–3(d), respectively. From the switching region (Region i and ii), we can see that the switching was a smooth process. There are no dramatic changes or optical rogue waves in the spectra and pulse energy, which is easy to arise in the build-up progress of breathing dissipative soliton [14]. Only a slight fluctuation in the spectra cross about 400 round trips before and after the switching points is observed, which indicates a quick and smooth switching.

To quantificationally compare the similarity of the spectral behaviors between the CW and CCW solitons during the switching process, the spectral correlations of two directions can be calculated by the equation [19]:

$$\rho(R_{cc}, R_c) = \frac{\left(\int I(\lambda, R_c) I(\lambda, R_{cc}) d\lambda\right)^2}{\int (I(\lambda, R_c))^2 d\lambda \int (I(\lambda, R_{cc}))^2 d\lambda},$$

where $I(\lambda, R_c)$ and $I(\lambda, R_{cc})$ are the spectral intensities at the wavelength of λ with the round trip number of R_c (CW soliton) and R_{cc} (CCW soliton), respectively. $\rho(R_{cc}, R_c)$ is the correlation value between the CW and CCW solitons (in the round trip number of R_c and R_{cc}, respectively), which can be determined by both of the similarity degrees of the spectral energy and spectral shape. When the value is close to 1, the spectral similarity will be high. Figures 3(e)–3(g) are the correlation maps of the CW and CCW solitons, corresponding to Figs. 3(b)–3(d), respectively. The similarity of the spectral behaviors of switching dynamics between the asynchronous dual-comb state and the synchronous breathing state are shown in Figs. 3(e) and 3(g), where four different regions including dual-comb & breathing, breathing & breathing, dual-comb & dual comb, and breathing & dual-comb are observed. The correlation values for asynchronous operation are lower than that of synchronous operation, which means that bidirectional solitons are transferred from small similarity for the asynchronous operation to high similarity for synchronous operation. The correlation values for synchronous operations (breathing & breathing or breathing & dual-comb) are over 0.9, indicating a high spectral similarity between the two directions. When the bidirectional laser operates in the dual-comb state, the correlation value is almost constant along with the round trips, indicating that the single-shot spectra are almost unchanged. However, in the breathing state, a slight periodical jitter was induced to the correlation values. When the CW (CCW) soliton is breathing, the correlation value jitters along with vertical (horizontal) directions in the maps, indicating that the spectral correlation between the CW and CCW solitons will be synchronously influenced by the soliton breathing. The spectral similarity characterization gives insight to fully understand the transient dynamics between asynchronous and synchronous operations, which can also be applied in other bidirectional cavity systems.

B. Stable asynchronous mode-locking operation

An asynchronous mode-locked laser is a promising source for dual-comb generation and dual-comb spectroscopy. In a bidirectional laser cavity, the asynchronous mode-locking operation can be realized by precisely adjusting the pump power and polarization state of the light. In this proposed laser cavity, when increasing the pump power of LD2 to 8 mW, the stable asynchronous mode-locking operation with a single pulse in both directions can be established. As shown in Fig. 4(a), the output spectra of the CW and CCW pulses have similar profiles but have different central wavelengths due to the difference in round-trip time of the two pulses [16]. The central wavelengths and 3 dB bandwidths of both solitons are 1558.59 and 8.52 nm (CW), 1559.63 and 8.1 nm (CCW), respectively. Stable soliton mode-locking is characterized by the clear Kelly sidebands on the spectra, which corresponds to anomalous cavity dispersion. The temporal pulse trains with a round-trip time difference $1/\Delta f_r$ of about 18.4 ms are shown in Fig. 4(b). As shown in Fig. 4(c), the repetition rate of CCW pulses is 43.327 65 MHz and has a 54.33-Hz difference with that of CW pulses, indicating that the fundamental frequency has different group velocities in the cavity. The autocorrelation traces of the CW and CCW pulses are shown in Fig. 4(d). By using a sech^2 fit, the pulse durations with little different chirps are estimated as 447 and 574 fs, respectively.

The coherence between two asynchronous solitons is an important parameter of a dual-comb laser source for

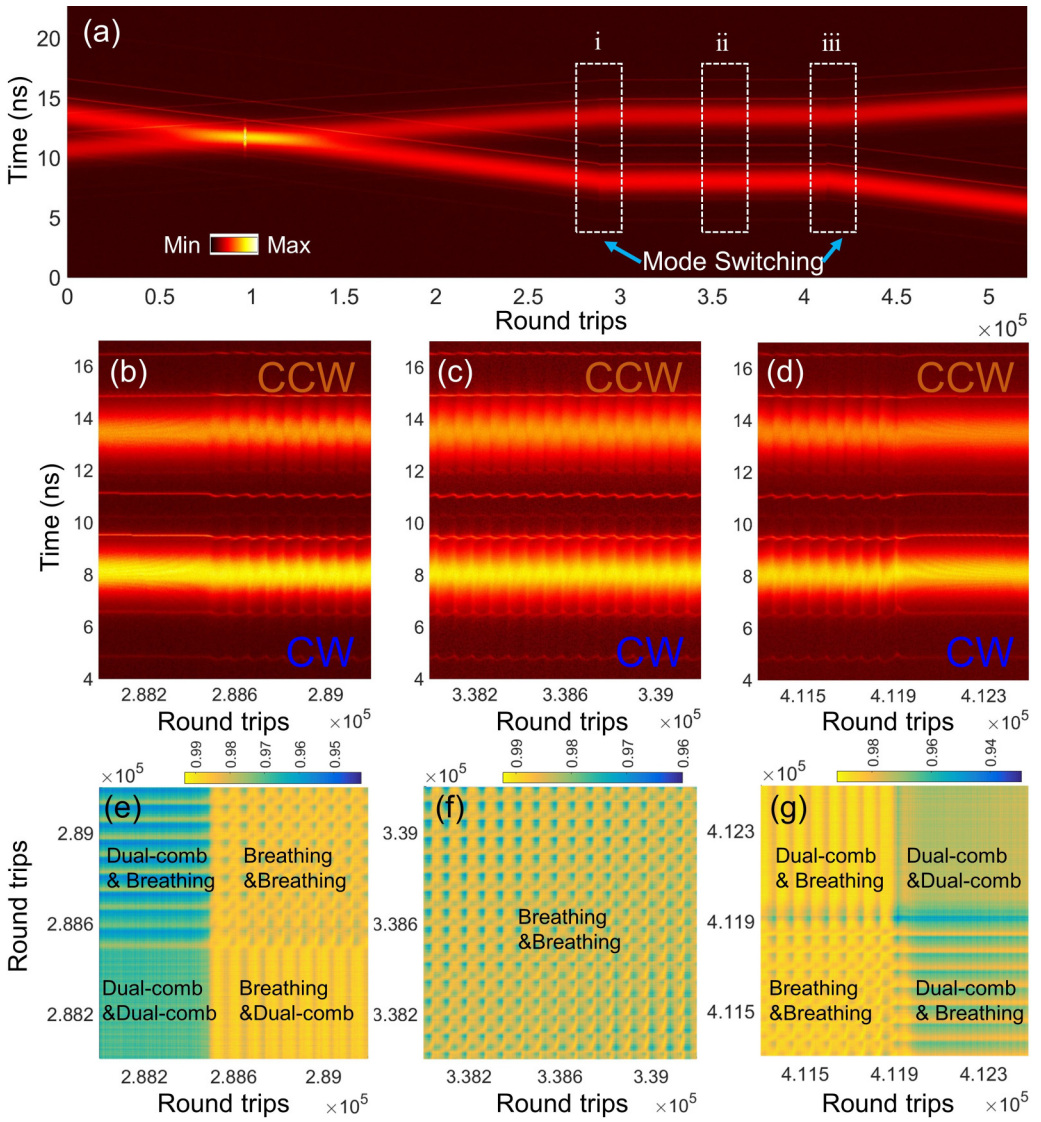

FIG. 3. (a) The spectral evolution involves the transient switching with 0.087-nm resolution. (Region i and iii represent the switching process, region ii represents the stable synchronous state). (b)–(d) Zoom-in view of the spectral evolution in region i, ii, and iii of (a), respectively. (e)–(g) 2D maps of spectral cross-correlation between the CW and CCW solitons corresponding to (b), (c), and (d), respectively.

interferometry applications. A traditional method to measure coherence is to record the difference in repetition rates in a long time [9]. TS-DFT makes it possible to obtain the single-shot spectrum with high resolution and has been widely applied to study the dynamics of ultrafast lasers. Here, we propose to obtain the real-time relative timing and phase information of two solitons by using the TS-DFT and spectral interferometry [6]. Figure 5(a) shows the spectral evolution for both CW and CCW pulses in the time domain at the repetition rate of 43.327 65 MHz over 80 000 consecutive round trips. The spectra of CW and CCW gradually approach each other and then walk off due to different repetition rates. Especially, a series of interferograms is observed in the regime of soliton collision, the zoom-in view of which is shown in Fig. 5(b). We can see obvious modulated spectral fringes across about 1400 round trips. Field autocorrelation trace in the collision regime according to the Wiener-Khinchin theorem [20] is shown in Fig. 5(d). Bidirectional solitons approach and separate each other via nearly fixed steps with symmetrical tendency, which indicates a small fluctuation of the difference of repetition rates. The largest recognizable separation is about 22 ps, which is mainly limited by the sampling system. The mutual coherence between two asynchronous laser trains is also presented in Figs. 5(c) and 5(e) by calculating the relative phase and mapping the dynamics of the soliton collision formation. As shown in Fig. 5(c), the phase evolution approaches a highly stable and linear shift in time, which is similar to the results in previous reported bound-state solitons [15]. The number of round trips per 2pi-cycle was about 87, indicating rapid phase dynamics between two solitons. The interaction planes over round trips in Fig. 5(e) reveal linear evolution in both separation and relative phase with negligible fluctuations. These results provide us with insight to study the mutual coherence between two asynchronous solitons.

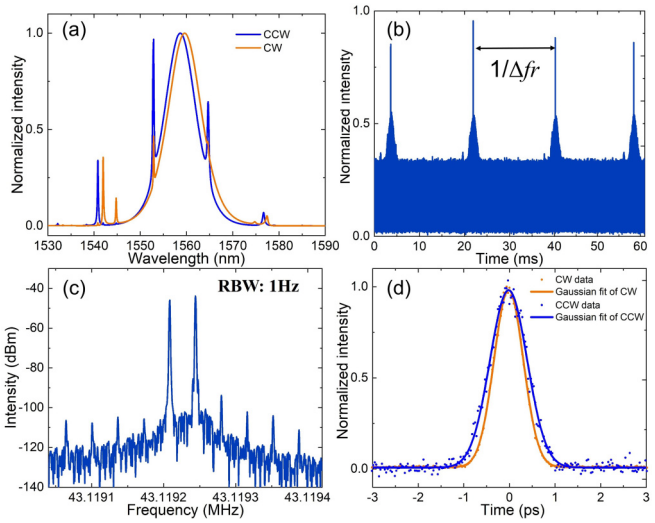

FIG. 4. Static properties of the asynchronous mode-locking operation. (a) Optical spectra of the CW and CCW pulses. (b) Temporal pulse trains within 60 ms span. (c) RF spectrum. (d) Autocorrelation traces of the CW and CCW pulses.

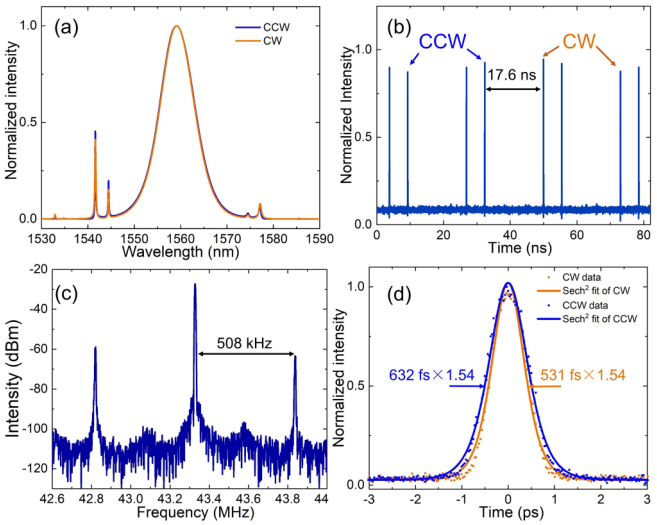

FIG. 6. Static properties of the breathing synchronous mode-locking operation. (a) Optical spectra of the CW and CCW pulses. (b) Temporal pulse trains. (c) RF spectrum. (d) Autocorrelation traces.

C. Breathing synchronous mode-locking operation

Through finely adjusting the pump power and the intracavity polarization state, the bidirectional fiber laser could switch to a breathing synchronous mode-locking state with the same repetition rate. It is found that once started, as the asynchronous operation, the laser can maintain stability at least for several hours. It is important to maintain a certain state with long-term stability for practical applications such as precision spectroscopy, distance measurement, and even 3D imaging. Both passive and active methods have been implemented to maintain the asynchronous state. To passively improve stability, vibration isolation, cavity integration, and temperature control can be used to make it immune to environmental changes. Meanwhile, by combining fast spectral analysis based on a time-stretched dispersion Fourier transform as the spectral discrimination criterion and intelligent polarization search algorithm, real-time control of the spectral width and shape of mode-locked femtosecond pulse be achieved [21].

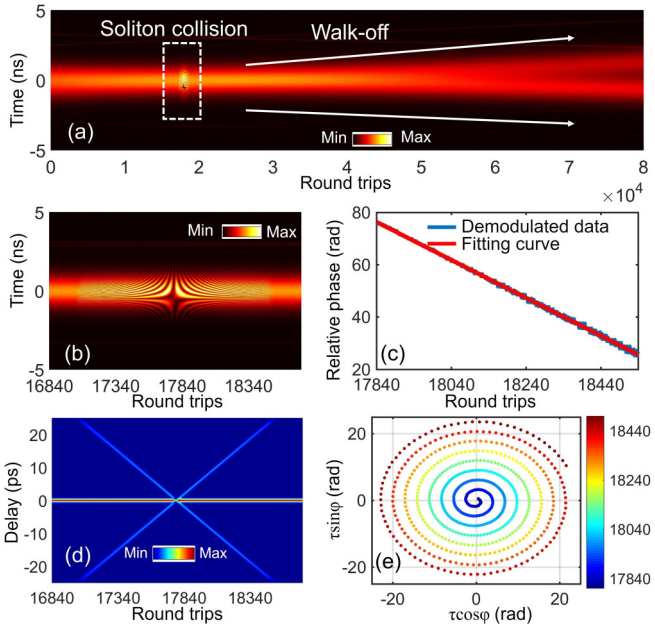

FIG. 5. Real-time dynamics of the asynchronous mode-locking operation. (a) The real-time spectral evolution along with the round trips. (b) Zoom-in view of soliton collision dynamics as the white dashed box indicated in (a). (c) Calculated relative phase of two solitons. (d) Field autocorrelation trace in the collision regime via Fourier transform. (e) Dynamics of the soliton collision formation mapped in the interaction plane over 1500 round trips. The radius and angle represent the pulse separation and relative phase, respectively.

In the breathing synchronous mode-locking state, the output spectra of the CW and CCW pulses present almost the same profiles with identical central wavelength and Kelly sidebands, as shown in Fig. 6(a). The 3-dB bandwidths of both solitons are 8.56 nm. The output power of CW is a little higher than that of CCW. The temporal pulse trains are shown in Fig. 6(b), indicating a constant temporal delay of 17.6 ns in every round trip. The delay is due to the collision between bidirectional solitons. According to our calculation, the collision point is inferred as the location of the CNT [15]. The oscillating pulse dynamics give rise to additional sidebands around the repetition rate with breathing frequency. The radio-frequency (RF) spectrum shown in Fig. 6(c) illustrates the fundamental repetition rate of about 43.327 992 MHz with an obvious satellite component, which agrees well with the breath frequency of 508 kHz. The autocorrelation traces of the CW and CCW pulses are shown in Fig. 6(d). By using a sech^2 fit, the pulse durations are estimated as 531 and 632 fs, respectively. Due to the asymmetry of cavity elements, pulses propagating in the CW and CCW directions pass through each element in reverse order and experience different cavity dispersion [10,22].

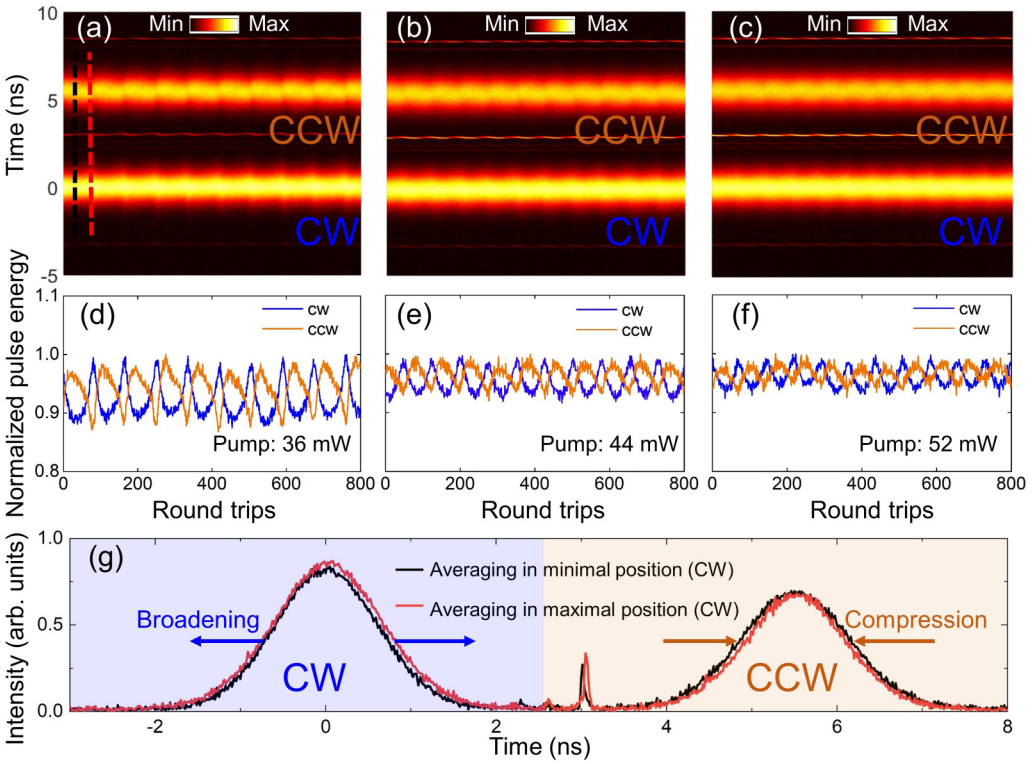

FIG. 7. Experimental real-time characterization of synchronous solitons. (a)–(c) Spectral evolution with different pump powers. (d)–(f) The evolution of calculated pulse energy with different pump powers. (g) Averaged single-shot spectra from the minimal and maximal positions of the envelope in (a).

Breathing synchronous solitons have complex and interesting dynamics, which is significant for the understanding of the fundamental mechanism in ultrafast optics. The real-time dynamics of breathing synchronous solitons are further explored as shown in Fig. 7. Figures 7(a)–7(c) show the spectral dynamics of counter-propagating solitons with clear breathing behavior at the pump power of 36, 44, and 52 mW, respectively. The parallel evolutions over round trips confirm the synchronization. Notably, even though the spectral evolution of CW and CCW pulses exhibit the same breathing period, the single-shot spectra of bidirectional solitons present antiphase breathing behavior. The operation at the pump power of 36 mW is illustrated as an example. There are about nine periods over round trips, corresponding to the breath period of 84 round trips, as shown in Fig. 7(a). The black (left) and red (right) dashed lines in Fig. 7(a) indicate the minimal (maximal) and maximal (minimal) positions for the CW (CCW) pulses in the first period, respectively. The single-shot spectra from both the minimal and maximal positions over nine periods are averaged and dedicated in Fig. 7(g) for composition. An obvious antiphase breathing behavior with spectral broaden for the CW pulses while spectral compression for the CCW pulses is observed. The corresponding single-shot pulse energy is also calculated by integrating its power spectral density over the whole wavelength band. The pulse energy dynamics for different pump powers are indicated in Figs. 7(d)–7(e). There is a pronounced energy exchange between the bidirectional solitons with the same period of spectral breathing. When increasing the pump power, both the spectrum and the energy modulation will become weak and even disappear, which is reversible. By decreasing the pump power, the stationary synchronous solitons will turn back to the breathing state. Thus, different from the synchronous breathing in the net-normal dispersion bidirectional laser [14], both the spectra and pulse energy in our scheme present opposite breathing behaviors over round trips for two directions, demonstrating the net cavity dispersion will influence the soliton dynamics.

Pump power not only affects the dynamic evolution of the breathing solitons but also influences breathing frequency and strength. We measure the RF spectra by increasing the pump powers as shown in Fig. 8(a). We locked the pump power of LD1 at 28 mW and increased the pump power of LD2 from 8 to 26 mW. The frequency and magnitude differences between the fundamental frequency and satellite component are defined to be breathing frequency and the intensity-modulated reject ratio (IMRR), respectively. The calculated evolution traces of breathing frequency and IMRR with different pump powers are shown in Fig. 8(b). When increasing the pump power from 36 to 54 mW, both the breathing frequency and IMRR will firstly increase with the linear trend and then gradually reach a saturated state. At the higher pump power, the opposite breathing between the bidirectional solitons shows a higher breathing frequency and lower energy exchange, which corresponds to the results in Fig 7. The highest breathing frequency and IMRR are 594 kHz and 41.66 dB, respectively. By further increasing the pump power, the bidirectional laser could switch to a stable synchronous operation without breathing, which means synchronous solitons without energy exchange are obtained. It is worth noting that the energy

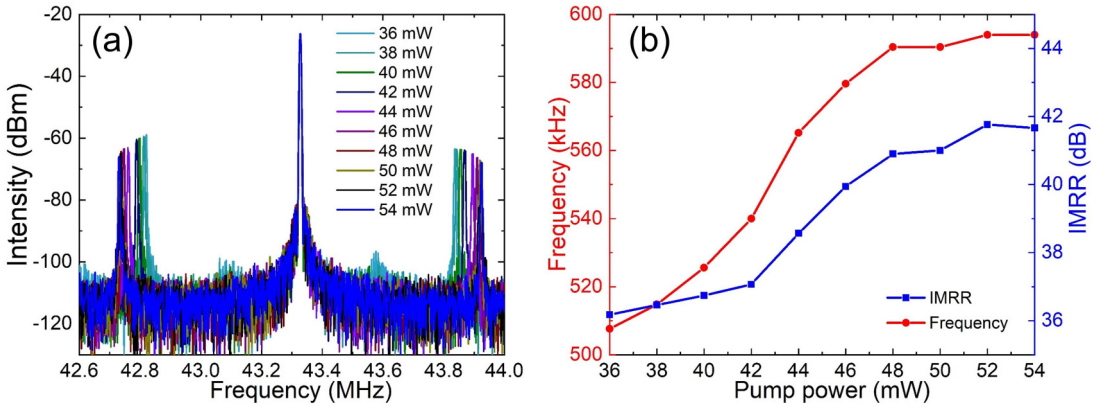

FIG. 8. (a) RF spectra with increasing the pump powers. (b) Evolution traces of breathing frequency and IMRR with different pump powers.

exchange was finished in the collide position where the CNT is located. When the laser operates in the asynchronous mode, the bidirectional solitons will collide with each other at different positions in every round trip instead of locking at the CNT to achieve periodic energy exchange. Therefore, the breathing asynchronous operation cannot be obtained in the cavity.

IV. CONCLUSION

In conclusion, we have experimentally investigated the statistical and dynamical properties of a bidirectional ultrafast laser in three operation modes, including the stable asynchronous, breathing synchronous, and transient switching operations. By combining the TS-DFT and spectral interferometry methods, transient switching dynamics are demonstrated with a switchable and weak interaction as well as spectral similarity change between counter-propagating solitons. The real-time relative timing and phase information between two solitons in the asynchronous mode are achieved, proving the mutual coherence between two laser trains. The captured evolution dynamics of both spectrum and energy modulation for breathing synchronous solitons exhibit opposite behavior, which indicates pronounced energy exchange in the breathing behavior. The comprehensive demonstration and understanding of the dynamics will contribute to applying bidirectional ultrafast lasers as versatile tools for dual-comb spectroscopy and a range of emerging applications.

ACKNOWLEDGMENTS

This work was supported by the National Key R&D Program of China (2020YFB1805901); National Natural Science Foundation of China (62105274); Technology and Innovation Commission of Shenzhen Municipality (SGDX2019081623060558, JCYJ20210324133406018); Guangdong Basic and Applied Basic Research Foundation (2021A1515012544); and Research Grants Council, University Grants Committee of Hong Kong SAR (PolyU152241/18E).

[1] G. Herink, B. Jalali, C. Ropers, and D. Solli, Resolving the buildup of femtosecond mode-locking with single-shot spectroscopy at 90 MHz frame rate, Nat. Photonics **10**, 321 (2016).

[2] Y. Luo, W. Ni, P. P. Shum, R. Xia, X. Tang, L. Zhao, and Q. Sun, Real-time spectral interferometry assisted recording of acoustic wave, in *Conference on Lasers and Electro-Optics, OSA Technical Digest* (Optica Publishing Group, Washington, DC, 2020), paper SF3P.2. https://ieeexplore.ieee.org/abstract/document/9193423

[3] A. F. J. Runge, N. G. R. Broderick, and M. Erkintalo, Observation of soliton explosions in a passively mode-locked fiber laser, Optica **2**, 36 (2015).

[4] X. Liu, D. Popa, and N. Akhmediev, Revealing the Transition Dynamics from Q Switching to Mode Locking in A Soliton Laser, Phys. Rev. Lett. **123**, 093901 (2019).

[5] D. R. Solli, C. Ropers, P. Koonath, and B. Jalali, Optical rogue waves, Nature (London) **450**, 1054 (2007).

[6] G. Herink, F. Kurtz, B. Jalali, D. R. Solli, and C. Ropers, Real-time spectral interferometry probes the internal dynamics of femtosecond soliton molecules, Science **356**, 50 (2017).

[7] J. Peng, Z. Zhao, S. Boscolo, C. Finot, S. Sugavanam, D. V. Churkin, and H. Zeng, Breather molecular complexes in a passively mode-locked fiber laser, Laser Photonics Rev. **15**, 2000132 (2021).

[8] J. Peng, S. Boscolo, Z. Zhao, and H. Zeng, Breathing dissipative solitons in mode-locked fiber lasers, Sci. Adv. **5**, eaax1110 (2019).

[9] T. Ideguchi, T. Nakamura, Y. Kobayashi, and K. Goda, Kerr-lens mode-locked bidirectional dual-comb ring laser for broadband dual-comb spectroscopy, Optica **3**, 748 (2016).

[10] Q. Yang, X. Yi, K. Yang, and K. Vahala, Counter-propagating solitons in microresonators, Nat. Photonics **11**, 560 (2017).

[11] S. Mehravar, R. A. Norwood, N. Peyghambarian, and K. Kieu, Real-time dual-comb spectroscopy with a free-running bidirectionally mode-locked fiber laser, Appl. Phys. Lett. **108**, 231104 (2016).

[12] J. Guo, Y. Ding, X. Xiao, L. Kong, and C. Yang, Multiplexed static FBG strain sensors by dual-comb spectroscopy with a free running fiber laser, Opt. Express **26**, 16147 (2018).

[13] Y. Yu, C. Kong, B. Li, J. Kang, Y. Ren, Z. Luo, and K. K. Wong, Behavioral similarity of dissipative solitons in an ultrafast fiber laser, Opt. Lett. **44**, 4813 (2019).

[14] Y. Zhou, Y. Ren, J. Shi, and K. Y. Wong, Breathing dissipative soliton explosions in a bidirectional ultrafast fiber laser, Photon. Res. **8**, 1566 (2020).

[15] I. Kudelin, S. Sugavanam, and M. Chernysheva, Build-up dynamics in bidirectional soliton fibre laser, Photon. Res. **8**, 776 (2020).

[16] C. Zeng, X. Liu, and L. Yun, Bidirectional fiber soliton laser mode-locked by single-wall carbon nanotubes, Opt. Express **21**, 18937 (2013).

[17] K. Yang, T. Li, X. Li, J. Chen, M. Liu, H. Cui, A. Luo, W. Xu, and Z. Luo, Mutually induced soliton polarization instability in a bidirectional ultrafast fiber laser, Opt. Lett. **46**, 4848 (2021).

[18] See Supplemental Material at http://link.aps.org/supplemental/10.1103/PhysRevA.105.043515 for a visual record of the transient switching process between asynchronous and synchronous modes.

[19] I. Kudelin, S. Sugavanam, and M. Chernysheva, Correlation of solitons in bidirectional mode-locked fibre laser, *Nonlinear Optics and Its Applications* (SPIE, New York, 2020), p. 11358.

[20] J. Peng, M. Sorokina, S. Sugavanam, N. Tarasov, D. V. Churkin, S. K. Turitsyn, and H. Zeng, Real-time observation of dissipative soliton formation in nonlinear polarization rotation mode-locked fibre lasers, Commun. Phys. **1**, 20 (2018).

[21] G. Pu, L. Yi, L. Zhang, C. Luo, Z. Li, and W. Hu, Intelligent control of mode-locked femtosecond pulses by time-stretch-assisted real-time spectral analysis, Light: Sci. Appl. **9**, 13 (2020).

[22] K. Kieu and M. Mansuripur, All-fiber bidirectional passively mode-locked ring laser, Opt. Lett. **33**, 64 (2008).